

Theoretical underpinnings of CP-Violation at the High-energy Frontier

Shaouly Bar-Shalom,^{1,*} Amarjit Soni,^{2,†} and Jose Wudka^{3,‡}

¹*Physics Department, Technion–Institute of Technology, Haifa 3200003, Israel*

²*Physics Department, Brookhaven National Laboratory, Upton, NY 11973, USA*

³*Physics Department, University of California, Riverside, CA 92521, USA*

(Dated: July 30, 2024)

We present a general analysis for the discovery potential of CP-violation (CPV) searches in scattering processes at TeV-scale colliders in an effective field theory framework, using the SMEFT basis for higher dimensional operators. In particular, we systematically examine the CP-violating sector of the SMEFT framework in some well motivated limiting cases, based on flavour symmetries of the underlying heavy theory. We show that, under naturalness arguments of the underlying new physics (NP) and in the absence of (or suppressed) flavour-changing interactions, there is only a single operator, $Q_{t\phi} = \phi^\dagger \phi (\bar{q}_{3t}) \tilde{\phi}$ which alters the top-Yukawa coupling, that can generate a non-vanishing CP-violating effect from tree-level SM×NP interference terms. We find, however, that CPV from $Q_{t\phi} = \phi^\dagger \phi (\bar{q}_{3t}) \tilde{\phi}$ is expected to be at best of $O(1\%)$ and, therefore, very challenging if at all measurable at the LHC or other future high-energy colliders. We then conclude that a potentially measurable CP-violating effect of $O(10\%)$ can arise in high-energy scattering processes *only* if flavour-changing interactions are present in the underlying NP; in this case a sizable CPV can be generated at the tree-level by pure NP×NP effects and not from SM×NP interference. We provide several examples of CPV at the LHC and at a future e^+e^- collider to support these statements.

arXiv:2407.19021v1 [hep-ph] 26 Jul 2024

* shaouly@physics.technion.ac.il

† adlsoni@gmail.com

‡ jose.wudka@ucr.edu

I. INTRODUCTION

One of the most important components of particle physics is CP-violation (CPV), since it is a key ingredient of the evolution of the universe and of the cosmological model [1–3]. It has been observed in K , D and B meson mixing and decays, where all observed CP asymmetries in those systems are found to be consistent with the Kobayashi-Maskawa mechanism for CPV in the Standard Model (SM) [4], which, however, seems insufficient for explaining the observed baryon asymmetry of the universe (BAU), see e.g., [5–7]. An extremely important consequence of these observations of CP violation is that CP is therefore not a symmetry of nature. It is, therefore, natural to expect new Beyond the SM (BSM) CP-odd phase(s).

It is for that reason that searches for new BSM CPV sources may be the pathway to a deeper understanding of particle physics and of the evolution of the observed universe. Given that no new physics (NP) has been detected yet up to the TeV scale, an important testing ground for BSM CPV effects is high-energy (multi-TeV scale) colliders, since CPV effects from an underlying heavy NP is suppressed by inverse powers of its scale. In particular, the NP that underlies the SM can be parameterized in general by higher dimensional, gauge-invariant effective operators, $Q_i^{(n)}$, in the so-called SM Effective Field Theory (SMEFT) framework, where the effective operators are constructed using the SM fields and their coefficients are suppressed by inverse powers of the NP scale Λ [8–12]:

$$\mathcal{L} = \mathcal{L}_{SM} + \sum_{n=5}^{\infty} \frac{1}{\Lambda^{n-4}} \sum_i \alpha_i Q_i^{(n)}, \quad (1)$$

where n is the mass dimension of $Q_i^{(n)}$ and we assume decoupling and weakly-coupled heavy NP, so that n equals the canonical dimension. One can further divide the higher-dimension effective operators to those that can be potentially generated at tree-level (PTG) and/or are loop generated (LG) in the underlying heavy theory [13]. The dominating NP effects are then expected to be generated by contributing operators with the lowest dimension (smallest n) that are PTG in the underlying heavy theory. Furthermore, the (Wilson) coefficients α_i depend on the details of the underlying heavy theory and, therefore, they parameterize all possible weakly-interacting and decoupling types of heavy physics. In particular, it is expected that $\alpha_i = O(1)$ for the PTG operators and $\alpha_i \sim 1/(4\pi)^2$ if the operators are LG; the LG operators are thus a-priori suppressed by a loop factor and, therefore, their effects at lower energies (i.e., $E < \Lambda$) are expected to be subleading.

In this paper we will characterize and identify the possible manifestations of new CPV sources from generic decoupling and weakly-coupled underlying heavy NP, using the SMEFT framework and exploiting the properties of the SM and SMEFT framework as well as the possible flavor structures of the underlying heavy physics. We will show that high-energy scattering processes involving the top-quark are the best and possibly *only* candidates for hunting BSM sources of CPV. Indeed, the top-quark, because of its relatively large mass, is expected to be more sensitive to TeV-scale NP and to CPV from BSM sources [14]; besides, CPV effects in top-quark systems from the SM CKM CP-odd phase are expected to be un-observably small [14].

In particular, we show that if flavor violation is suppressed in the underlying heavy theory, then only a single operator that involves the top-quark and Higgs fields can potentially yield non-negligible CPV which is, however, still below the expected sensitivity of the LHC and/or future high-energy colliders. On the other hand, if the underlying heavy theory contains flavor violating $t \rightarrow u$ and/or $t \rightarrow c$ transitions, then sizable tree-level CPV of $O(10\%)$ can be generated, that is within the reach of e.g., the LHC.

II. PATTERS OF CP-VIOLATION IN THE SMEFT

We divide the CPV SMEFT sector into two groups: CPV operators that can generate $O(1/\Lambda^2)$ interference effects with the SM,¹ and those that cannot interfere with the SM to this order when CKM suppression factors are ignored. The first group can be further subdivided depending on whether the interference with the SM is proportional to the fermion masses or is not, while the second group consists of flavor-changing operators.²

¹ We will ignore the single dimension 5 operator in SMEFT since it is lepton-number violating and its scale is accordingly expected to be very high; we also ignore operators of dimension ≥ 7 since they are suppressed by higher powers of the NP scale Λ .

² Other classifications of the CP-odd sector in the SMEFT framework, based on similar arguments, can be found in [15–17].

A. CPV from interference with the SM

In order to understand the patterns of CPV through interference with the SM, it is useful to consider two limiting cases of the SM that are well motivated phenomenologically and experimentally:

SM₀: all masses in the SM are set to zero, so that the fermion sector is segregated into a number of non-interacting sub-sectors, each labeled by its flavor and chirality. This theory has a $\mathcal{G}_0 = U(3)^5$ global flavor symmetry (without right-handed neutrinos) and it is CP-invariant (except for a possible strong CP θ -term [18] that we ignore). Note that this limit motivated the so-called Minimal Flavor Violation (MFV) ansatz for model building of NP beyond the SM, where the Yukawa couplings are promoted to spurion fields [19, 20].

SM_t: The SM₀ with a massive top-quark. That is:

$$\mathcal{L}_{\text{SM}_t} = \mathcal{L}_{\text{SM}_0} + \left(y_t \bar{q}_3 t \tilde{\phi} + \text{H.c.} \right), \quad (2)$$

where q_3 denotes the third-generation left-handed quark isodoublet, t the right-handed top-quark isosinglet and ϕ is the SM Higgs field. The SM_t has a reduced symmetry $\mathcal{G}_t = U(3)^4 \times U(2) \times U(1) \subset \mathcal{G}_0$ and it can give rise to “new” processes compared to those described by the SM₀, with amplitudes proportional to a power of y_t .

The higher dimensional effective operators of the SMEFT can likewise be segregated into the sectors that possess the \mathcal{G}_0 and \mathcal{G}_t global symmetries of the SM₀ and SM_t, respectively. We denote by SMEFT₀ the terms in SMEFT that are invariant under \mathcal{G}_0 and by SMEFT_t those that are invariant under \mathcal{G}_t but not contained in SMEFT₀. Note that, in contrast with SM₀, SMEFT₀ contains CPV interactions (see below). The corresponding \mathcal{G}_0 and \mathcal{G}_t -symmetric effective Lagrangians are then:

$$\begin{aligned} \mathcal{L}_{\mathcal{G}_0} &= \mathcal{L}_{\text{SM}_0} + \mathcal{L}_{\text{SMEFT}_0}, \\ \mathcal{L}_{\mathcal{G}_t} &= \mathcal{L}_{\text{SM}_t} + \mathcal{L}_{\text{SMEFT}_0} + \mathcal{L}_{\text{SMEFT}_t}. \end{aligned} \quad (3)$$

It then follows that only operators in SMEFT₀ will interfere with the SM₀. This implies that CPV interference effects between the SMEFT and the SM that are generated by operators *not* in SMEFT₀ will be suppressed by at least one power of a fermion mass; of these the dominant ones will be those for which this suppression is $\propto m_t$, and these are generated by SMEFT_t.

In Table I we list the complete set of potentially CPV dimension six effective operators of the SMEFT₀ and SMEFT_t sectors. Note that the CPV operators of the SMEFT₀ sector do not involve fermion fields and they are all LG in the underlying heavy theory. In the SMEFT_t sector, only the operator $Q_{t\phi}$ is PTG. Moreover, the LG operators of the SMEFT₀ sector (as well as the operator Q_{tG} in the SMEFT_t sector) are tightly constrained by the lepton and neutron electric dipole moments [21]. It thus follows that the leading CPV effect from interference with the SM is generated by $Q_{t\phi}$, which is the only PTG operator in the SMEFT_t sector; all other operators that interfere with the SM will yield CPV which is either loop suppressed (from LG operators) or suppressed by powers of light fermion masses.

TABLE I: The dimension six CPV effective operators of the SMEFT₀ and SMEFT_t sectors, where q_3 is the left-handed SU(2) doublet of the 3rd generation quarks and t is the right-handed top-quark singlet.

$\mathcal{L}_{\text{SMEFT}_0}^{\text{CPV}}$	$\mathcal{L}_{\text{SMEFT}_t}^{\text{CPV}}$
$Q_{\tilde{G}} = f^{ABC} \tilde{G}_{\mu}^{A\nu} G_{\nu}^{B\rho} G_{\rho}^{C\mu}$	$Q_{tG} = (\bar{q}_3 \sigma^{\mu\nu} T^A t) \tilde{\phi} G_{\mu\nu}^A$
$Q_{\tilde{W}} = f^{IJK} \tilde{G}_{\mu}^{I\nu} W_{\nu}^{J\rho} W_{\rho}^{K\mu}$	$Q_{tW} = (\bar{q}_3 \sigma^{\mu\nu} t) \tau^I \tilde{\phi} W_{\mu\nu}^I$
$Q_{\phi\tilde{G}} = \phi^\dagger \phi \tilde{G}_{\mu\nu}^A G^{A\mu\nu}$	$Q_{tB} = (\bar{q}_3 \sigma^{\mu\nu} t) \tilde{\phi} B_{\mu\nu}$
$Q_{\phi\tilde{W}} = \phi^\dagger \phi \tilde{W}_{\mu\nu}^I G^{I\mu\nu}$	$Q_{t\phi} = \phi^\dagger \phi (\bar{q}_3 t) \tilde{\phi}$
$Q_{\phi\tilde{B}} = \phi^\dagger \phi \tilde{B}_{\mu\nu} B^{\mu\nu}$	
$Q_{\phi\tilde{W}B} = \phi^\dagger \tau^I \phi \tilde{W}_{\mu\nu}^I B^{\mu\nu}$	

B. CPV from NP×NP terms

All non-Hermitian operators will have in general complex Wilson coefficients and can, therefore, generate CPV effects. As explained above, if the operators do not belong to the SMEFT₀ and SMEFT_t sectors, then CPV from SM×NP interference effects are negligible, but CPV from NP×NP effects may still be significant.

In particular, it is worth listing here the non-hermitian operators that can in principle carry a CP-odd phase without flavor-violation in the underlying physics. These include the flavor-diagonal operators in $\mathcal{L}_{\text{SMEFT}_t}^{\text{CPV}}$ (see Table I) extended to all fermion species as well as the following PTG flavor-diagonal operators:

$$\begin{aligned}
Q_{\phi ud} &= i \left(\tilde{\phi}^\dagger D_\mu \phi \right) (\bar{u} \gamma^\mu d) , \\
Q_{\ell edq} &= (\bar{\ell}^j e) (\bar{d} q_j) , \\
Q_{\ell equ}^{(1)} &= (\bar{\ell}^j e) \epsilon_{jk} (\bar{q}^k u) , \\
Q_{\ell equ}^{(3)} &= (\bar{\ell}^j \sigma_{\mu\nu} e) \epsilon_{jk} (\bar{q}^k \sigma^{\mu\nu} u) , \\
Q_{quqd}^{(1)} &= (\bar{q}^j u) \epsilon_{jk} (\bar{q}^k d) , \\
Q_{quqd}^{(8)} &= (\bar{q}^j T^a u) \epsilon_{jk} (\bar{q}^k T^a d) ,
\end{aligned} \tag{4}$$

where j, k are SU(2) indices and ℓ, e denote the lepton fields in same generation and, similarly, q, u, d are quark fields of a single generation. These operators do not conserve the global \mathcal{G}_0 and \mathcal{G}_t symmetries mentioned above so that their interference effects with the SM are suppressed by powers of m/Λ , where m is a *light* fermion mass and, therefore, they are unobservable (this is the case for both CPV and CP-conserving (CPC) reactions). The leading CPV effects in this case will potentially arise from interference between different NP contributions, which we denote as NP² effects that are $O(1/\Lambda^4)$ (this is also the case if the underlying heavy theory induces flavor-violating SMEFT operators), which limits the sensitivity of the LHC to such effects (see below).

Finally, if flavor is violated in the underlying heavy theory, then all SMEFT operators containing flavor-violating combinations of fermion fields can violate CP. These operators cannot interfere at tree-level with the SM (when the small off-diagonal CKM effects are ignored), so that the leading CPV effects in this case will again be generated from NP² terms, e.g., CPV effects from 4-fermion operators with generic flavor indices that we discuss in some detail below.

III. CP-VIOLATION IN HIGH-ENERGY SCATTERING PROCESSES

The differential cross-section for any given scattering process may be divided into its CPV and CPC parts:

$$d\sigma \equiv d\sigma_{\text{CPC}} + d\sigma_{\text{CPV}} . \tag{5}$$

In terms of these, the generic form of an observable sensitive to the corresponding CPV effects will be necessarily proportional to the ratio between the CPV and CPC terms:

$$\mathcal{A}_{\text{CP}} \propto \frac{d\sigma_{\text{CPV}}}{d\sigma_{\text{CPC}}} , \tag{6}$$

so that it scales with the CPV contribution to the cross-section, $d\sigma_{\text{CPV}}$, while being suppressed by the CPC terms of the corresponding cross-section, $d\sigma_{\text{CPC}}$.

Now, in order for a processes to violate CP, there must be at least two contributing amplitudes with different phases:

$$\mathcal{M}_{i \rightarrow f} = M_1 e^{i(\phi_1 + \delta_1)} + M_2 e^{i(\phi_2 + \delta_2)} , \tag{7}$$

where we have factored out the CP-odd and CP-even phases, $\phi_{1,2}$ and $\delta_{1,2}$, respectively; the latter arise from final state interactions (FSI) at higher loop orders (when no resonances are involved, which is the working assumption within the SMEFT framework). If the process under consideration is not self-conjugate, then the amplitude for the charge-conjugate (CC) channel ($\mathcal{M}_{\bar{i} \rightarrow \bar{f}}$) is obtained from (7) by changing the sign of the CP-odd phases $\phi_i \rightarrow -\phi_i$ and replacing $M_i \rightarrow M_i^*$. The CC reaction is useful in constructing CPV observables in the presence of CP-even phases (see Sect. IIIB).

We are interested in studying the leading CPV effects, so we will consider below only the cases where both M_1 and

M_2 are generated at tree-level,³ in which case the CP-even phases vanish: $\delta_i = 0$.

A. Patterns of CP-Violation

When considering only tree-level effects (i.e., no CP-even phases from FSI) and ignoring light quark masses, the general form of the amplitude, in the presence of the dim.6 SMEFT operators, takes the form

$$\mathcal{M}_{i \rightarrow f} = M_{\text{SM}} + \sum_k \frac{|\alpha_k|}{\Lambda^2} M_k e^{i\phi_k} + \dots \quad (8)$$

where α_k are the Wilson coefficient defined in Eq. 1 and the CPV phases (ϕ_k) in α_k are factored out and explicitly displayed. The ellipsis denote contributions from higher dimensional operators.

Using the generic form of the NP amplitude in Eq. 8, we can now categorize *all possible* tree-level CPV manifestations that can be generated by the SMEFT in high-energy scattering processes, and estimate their magnitude. Recall that if the underlying heavy NP is natural, then we expect $\alpha_k \sim 1$ for PTG operators and $\alpha_k \sim 1/(16\pi^2)$ for LG operators [13]. Therefore, the leading CPV effects are expected to arise from PTG operators, and they can be of 3 types:

- **TLCPV-I:** If there is SM-SMEFT interference. In this case, we argued above that there is only one PTG operator that can contribute, $Q_{t\phi}$, so that (the ellipsis denote contributions $\propto 1/\Lambda^4$)

$$\begin{aligned} d\sigma_{\text{CPC}} &\propto |M_{\text{SM}}|^2 + \frac{|\alpha_{t\phi}|}{\Lambda^2} \text{Re} \left(M_{\text{SM}} M_{t\phi}^\dagger \right) \cos \phi_{t\phi} + \dots, \\ d\sigma_{\text{CPV}} &\propto \frac{|\alpha_{t\phi}|}{\Lambda^2} \text{Im} \left(M_{\text{SM}} M_{t\phi}^\dagger \right) \sin \phi_{t\phi} + \dots \end{aligned} \quad (9)$$

- **TLCPV-II:** If there is no SM-SMEFT interference (for dimension 6 operators and higher). In this case, the $1/\Lambda^4$ terms can be consistently retained (the ellipsis now denote terms $\propto 1/\Lambda^6$):

$$\begin{aligned} d\sigma_{\text{CPC}} &\propto |M_{\text{SM}}|^2 + \sum_k \frac{|\alpha_k|^2}{\Lambda^4} |M_k|^2 + \sum_{k<l} \frac{|\alpha_k \alpha_l|}{\Lambda^4} \text{Re} \left(M_k M_l^\dagger \right) \cos \Delta\phi_{kl} + \dots; \quad \Delta\phi_{kl} = \phi_k - \phi_l, \\ d\sigma_{\text{CPV}} &\propto \sum_{k<l} \frac{|\alpha_k \alpha_l|}{\Lambda^4} \text{Im} \left(M_k M_l^\dagger \right) \sin \Delta\phi_{kl} + \dots \end{aligned} \quad (10)$$

- **TLCPV-III:** If there is no SM contribution; so the relevant expressions are the previous ones with $M_{\text{SM}} = 0$.

The above expressions, in all cases, take the generic form (*cf.* Eq. 7)

$$d\sigma_{\text{CPC}} = c_1 |M_1|^2 + c_2 |M_2|^2 + c_3 \text{Re} \left(M_1 M_2^\dagger \right) \cos \Delta\phi, \quad (11)$$

$$d\sigma_{\text{CPV}} = c_4 \text{Im} \left(M_1 M_2^\dagger \right) \sin \Delta\phi, \quad (12)$$

so that $\Delta\phi$ denotes a CP-odd phase and the coefficients c_i have the following Λ dependence:

CPV type	c_1	c_2	c_3	c_4
TLCPV-I	1	$\frac{v^4}{\Lambda^4}$	$\frac{v^2}{\Lambda^2}$	$\frac{v^2}{\Lambda^2}$
TLCPV-II	1	$\frac{v_E^4}{\Lambda^4}$	$\frac{v_E^4}{\Lambda^4}$	$\frac{v_E^4}{\Lambda^4}$
TLCPV-III	$\frac{v_E^4}{\Lambda^4}$	$\frac{v_E^4}{\Lambda^4}$	$\frac{v_E^4}{\Lambda^4}$	$\frac{v_E^4}{\Lambda^4}$

where $v_E = v$ or $v_E = E$, depending on whether the SMEFT contributions give rise to an energy growing cross-section.

³ If M_i is generated at 1-loop it will be suppressed by an additional loop factor $\sim 1/(16\pi^2)$, with respect to the tree-level case.

Also, at tree-level (i.e., in the absence of FSI), the imaginary part of the interference term, $\text{Im} \left(M_1 M_2^\dagger \right)$, is necessarily proportional to a Levi-Civita tensor ($\epsilon_{\alpha\beta\gamma\delta}$) involving four independent momenta, so that the CPV term of the cross-section is in general:

$$d\sigma_{\text{CPV}} \propto c_4 \cdot \epsilon(u_1, u_2, u_3, u_4) \sin \Delta\phi, \quad (13)$$

where the u_i represent momenta or polarization/spin 4-vectors associated with the particles in the scattering process of interest and $\epsilon(u_1, u_2, u_3, u_4) = \epsilon_{\alpha\beta\gamma\delta} u_1^\alpha u_2^\beta u_3^\gamma u_4^\delta$. Note that $\epsilon(u_1, u_2, u_3, u_4)$ can always be expressed as a triple product $\vec{u}_i \cdot (\vec{u}_j \times \vec{u}_k)$ in some rest frame. Furthermore, to obtain a non-vanishing $\epsilon(u_1, u_2, u_3, u_4)$ requires at least 4 independent vectors, so that either there are at least 3 particles in the final state, i.e., $a + b \rightarrow 1 + 2 + 3$, or one must trace the spin/polarization information in a $2 \rightarrow 2$ scattering process.

A useful measure of the statistical significance, N_{SD} , with which an asymmetry \mathcal{A} can be detected in a given process with cross-section σ (ignoring systematic uncertainties) is provided by:

$$N_{SD}(\mathcal{A}) \sim \mathcal{A} \sqrt{\sigma \cdot \mathcal{L}}, \quad (14)$$

where \mathcal{L} is the available integrated luminosity. Referring to Eqs. 7, 11, 12 and 14, we summarize in Table II the characteristics and Λ dependence of the above three tree-level CPV scenarios, also addressing their potential observability N_{SD} . Evidently, scattering process with no SM contribution, where the NP yields a growing cross-section (TLCPV-III scenario), i.e., $\sigma \propto E^4/\Lambda^4$, are expected to be the most sensitive to BSM CPV effects. An example of such a process is given in Sect. V.

TABLE II: The Λ dependence of the CP-asymmetry \mathcal{A}_{CP} and its potential observability $N_{SD}(\mathcal{A}_{CP})$, as well as a description of the leading contributions to the CPV and CPC parts of the cross-section σ , for the three tree-level CPV scenarios TLCPV-I,II,III, where $v_E = v$ or $v_E = E$, depending on whether or not the SMEFT contributions give rise to an energy growing cross-section. See also text.

	CPV source in σ	Leading CPC term in σ	\mathcal{A}_{CP}	$N_{SD}(\mathcal{A}_{CP})$
TLCPV-I	$\text{Im} \left(M_{SM} M_{NP}^\dagger \right) \propto \frac{v^2}{\Lambda^2}$	$ M_{SM} ^2$	$\frac{v^2}{\Lambda^2}$	$\frac{v^2}{\Lambda^2}$
TLCPV-II	$\text{Im} \left(M_{NP'} M_{NP}^\dagger \right) \propto \frac{v_E^4}{\Lambda^4}$	$ M_{SM} ^2$	$\frac{v_E^4}{\Lambda^4}$	$\frac{v_E^4}{\Lambda^4}$
TLCPV-III	$\text{Im} \left(M'_{NP} M_{NP}^\dagger \right) \propto \frac{v_E^4}{\Lambda^4}$	$ M_{NP} ^2 \propto \frac{v_E^4}{\Lambda^4}$	1	$\frac{v_E^2}{\Lambda^2}$

B. Constructing observables for tree-level CP-Violation

We now consider $2 \rightarrow 3$ scattering processes of the form $ab \rightarrow 1 + 2 + 3$ (and the CC reaction $\bar{a}\bar{b} \rightarrow \bar{1} + \bar{2} + \bar{3}$) that are sensitive to CPV effects, and for which CPV observables can be constructed without the need to analyze the spin/helicity of the final particles. We note that, in general, CPC contributions to the cross sections that depend on the CP-even phases δ (*cf.* Eq. 7) may give rise to a fake CPV signal even if the CP-odd phases ϕ vanish, see [14, 22] and discussion below. Thus, the construction of genuine CPV observables requires the joint consideration of a reaction and its CC counterpart [22], as described below.

It is useful to classify CP observables according to their transformation properties under “naive time reversal” (T_N), where T_N : time \rightarrow $-$ time [14]. This classification is presented in Table III. In particular, a T_N -odd CP-odd observable requires only a CP-odd phase, which could arise already at the tree-level, while a T_N -even CP-odd observable needs also a non-vanishing CP-even phase from FSI (i.e., δ_i in Eq. 7), which is typically of a higher order. Thus, since T_N -odd CP-odd observables are sensitive to tree-level CPV, they are more likely to see sizable CPV signals, in some cases reaching $\gtrsim 10\%$, see e.g., [14, 23–25].

Thus, in order to probe tree-level CPV, in the $2 \rightarrow 3$ process $ab \rightarrow 1 + 2 + 3$ and the CC reaction $\bar{a}\bar{b} \rightarrow \bar{1} + \bar{2} + \bar{3}$, we will use the following T_N -odd momenta correlations:

$$\mathcal{O}_{\text{CP}} = \epsilon(p_a, p_1, p_2, p_3) \quad , \quad \overline{\mathcal{O}}_{\text{CP}} = \epsilon(p_{\bar{a}}, p_{\bar{1}}, p_{\bar{2}}, p_{\bar{3}}) \quad , \quad (15)$$

TABLE III: General classification of CP-odd observables, \mathcal{A}_{CP} , under naive time reversal T_N , where $\Delta\delta$ and $\Delta\phi$ denote the CP-even and CP-odd phases.

	T_N -odd (CP-odd)	T_N -odd (CP-even)
CP-asymmetry	$A_{CP} \propto \cos \Delta\delta \sin \Delta\phi$	$A_{CP} \propto \sin \Delta\delta \sin \Delta\phi$
Required phases	only CP-odd	Both CP-odd & CP-even
Sensitivity	tree-level CPV	CP-even phase from FSI (higher order effect)

which transform under C and CP as:

$$\begin{aligned} C(\mathcal{O}_{CP}) &= +\overline{\mathcal{O}_{CP}}, \quad C(\overline{\mathcal{O}_{CP}}) = +\mathcal{O}_{CP}, \\ CP(\mathcal{O}_{CP}) &= -\overline{\mathcal{O}_{CP}}, \quad CP(\overline{\mathcal{O}_{CP}}) = -\mathcal{O}_{CP}. \end{aligned} \quad (16)$$

Using the \mathcal{O}_{CP} 's in Eq. 15, we then define the following T_N -odd (and also P -violating) asymmetries:

$$A_T \equiv \frac{N(\mathcal{O}_{CP} > 0) - N(\mathcal{O}_{CP} < 0)}{N(\mathcal{O}_{CP} > 0) + N(\mathcal{O}_{CP} < 0)}, \quad (17)$$

$$\bar{A}_T \equiv \frac{N(-\overline{\mathcal{O}_{CP}} > 0) - N(-\overline{\mathcal{O}_{CP}} < 0)}{N(-\overline{\mathcal{O}_{CP}} > 0) + N(-\overline{\mathcal{O}_{CP}} < 0)}, \quad (18)$$

where $N(\mathcal{O}_{CP} > 0)$ is the number of events for which $\text{sign}(\mathcal{O}_{CP}) > 0$ is measured etc.

The asymmetries A_T and \bar{A}_T are sensitive to the CP-odd phase BUT are not proper CP-asymmetries, since they are not eigenstate of CP, i.e., $CP(A_T) = \bar{A}_T$. In particular, $A_T \propto \sin(\Delta\delta + \Delta\phi)$ and $\bar{A}_T \propto \sin(\Delta\delta - \Delta\phi)$ (see [25]), so that in general $A_T \neq 0$ and/or $\bar{A}_T \neq 0$ could be generated without CPV, i.e., if $\Delta\phi = 0$ and $\Delta\delta \neq 0$. Therefore, in order to isolate the pure CPV effects, we need to combine the information from both A_T and \bar{A}_T as follows:

$$\mathcal{A}_{CP} = \frac{1}{2} (A_T - \bar{A}_T). \quad (19)$$

As was shown in [25], when the initial state is not self-conjugate and its CC state has a different PDF, as can be the case at the LHC, i.e., $\text{PDF}(ab) \neq \text{PDF}(\bar{a}\bar{b})$, then a ‘‘fake’’ CP signal can still be generated in \mathcal{A}_{CP} in the presence of a CP-even phase, which is $\propto \cos \Delta\phi$. This is, however, not the case for the processes that we consider below as an example of tree-level CPV at the LHC (see Sect. IV B).

Finally, if the process under consideration is the same as the CC channel, i.e., $ab \rightarrow 1+2+3$ and $\bar{a}\bar{b} \rightarrow \bar{1}+\bar{2}+\bar{3}$ are the same (as is the case for example in $e^+e^- \rightarrow t\bar{t}h$ that we will consider below in Sect. IV A), then $\mathcal{A}_{CP} = A_T = \bar{A}_T$.

IV. CP-VIOLATION FROM SM \times NP INTERFERENCE

As explained in Sect. II A, there is a single dimension 6 PTG operator, $Q_{t\phi}$, that may give rise to non-negligible CPV effects through interference with the SM in high-energy scattering processes; this operator modifies the tth couplings and the interference effects will not be proportional to a light quark mass.

Given any model M , It is therefore convenient to parameterize the tth generic interaction as follows:

$$\mathcal{L}_M^{tth} = -h\bar{t}(a_M + ib_M\gamma_5)t, \quad (20)$$

allowing for both scalar and pseudo-scalar couplings of the top quark to the Higgs; in particular, for the SM,

$$\mathcal{L}_{SM}^{tth} = y_t h \bar{t}t \quad ; \quad y_t = \frac{m_t}{v}, \quad (21)$$

so that $a_{SM} = m_t/v \sim 1/\sqrt{2}$ ($v \sim 246$ GeV is the Higgs VEV), and $b_{SM} = 0$ (no pseudo-scalar coupling).

Considering now the SMEFT model $\mathcal{L}_{\mathcal{G}_t}$ of Eq. 3, which contains $Q_{t\phi}$, we find

$$\mathcal{L}_{\mathcal{G}_t}^{tth} = \frac{m_t}{v} h \bar{t} t + \frac{3v^2}{2\sqrt{2}\Lambda^2} h (\alpha_{t\phi} \bar{t} P_R t + \text{H.c.}) , \quad (22)$$

so that

$$\begin{aligned} a_{\mathcal{G}_t} &= a_{SM} + \frac{3}{2\sqrt{2}} \frac{v^2}{\Lambda^2} \text{Re}(\alpha_{t\phi}) , \\ b_{\mathcal{G}_t} &= \frac{3}{2\sqrt{2}} \frac{v^2}{\Lambda^2} \text{Im}(\alpha_{t\phi}) . \end{aligned} \quad (23)$$

Thus, with $\Lambda \sim 1$ TeV and a natural underlying heavy physics, i.e., $\text{Re}(\alpha_{t\phi}) \sim 1$ and $\text{Im}(\alpha_{t\phi}) \sim 1$, we have $a_{\mathcal{G}_t} \sim a_{SM} \sim 1/\sqrt{2}$ and a rather suppressed pseudo-scalar coupling $b_{\mathcal{G}_t} \sim 0.07$; in this case we expect small CPV effects at high-energy scattering processes, as will be verified below.

On the other hand, multi-Higgs extensions of the SM could naturally give rise to a sizable pseudo-scalar coupling, of the order of a_{SM} . This is the case, for example, in the two-Higgs doublet model (2HDM) with CPV (generated by the scalar potential, see e.g., [14]), where the lightest Higgs could have scalar and pseudo-scalar tth couplings of $O(a_{SM})$, i.e., $a_{2HDM}, b_{2HDM} \sim a_{SM} \sim 1/\sqrt{2}$; not a favorable scenario but not excluded experimentally [26–28].

We will discuss below three processes which can potentially yield a CPV signal at tree-level, originating from NP in tth interaction interfering with the SM at the tree-level: $e^+e^- \rightarrow t\bar{t}h$ at a future e^+e^- collider and two single-top – Higgs associated production processes at the LHC, $pp \rightarrow thW$ and $pp \rightarrow thj$, where j is a light-quark jet.

A. $e^+e^- \rightarrow t\bar{t}h$: CPV from tree-level interference at a future e^+e^- collider

Tree-level CP-violation in $e^+e^- \rightarrow t\bar{t}h$ was first studied in [23] (see also [14]), where CPV in the tth vertex was assumed to originate from a CP-odd phase in a 2HDM (similar tree-level CPV effects were also studied in [24] for the case of $e^+e^- \rightarrow t\bar{t}Z$). Here we will generalize the study in [23] to the EFT case, i.e., to any underlying heavy physics that can generate the CPV tth interaction of Eq. 20; in particular, discussing the expected CPV signal from the SMEFT operator $Q_{t\phi}$.

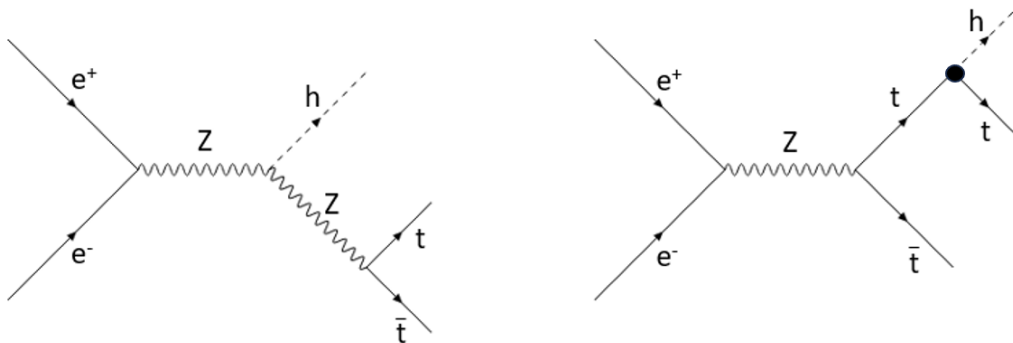


FIG. 1: Representative Feynman diagrams for the lowest order SM and NP contributions (marked by a heavy dot) to $e^+e^- \rightarrow t\bar{t}h$ at a future e^+e^- collider. Tree-level CP-violation arises from interference between these two diagrams. See also text.

In this process the tree-level CPV effect arises from interference between the diagrams in Fig. 1. To leading order in the SMEFT expansion, the CPV part of the differential cross-section (see Eq. 12) is (see also [14, 23]):

$$d\sigma_{CPV}^{tth} \propto m_t \cdot c_{hZZ} \cdot b_{\mathcal{G}_t} \cdot \epsilon(p_{e^-}, p_{e^+}, p_t, p_{\bar{t}}) , \quad (24)$$

where $b_{\mathcal{G}_t}$ is the pseudo-scalar tth coupling from the CPV SMEFT $_t$ sector (see Eq. 23), c_{hZZ} represents the hZZ

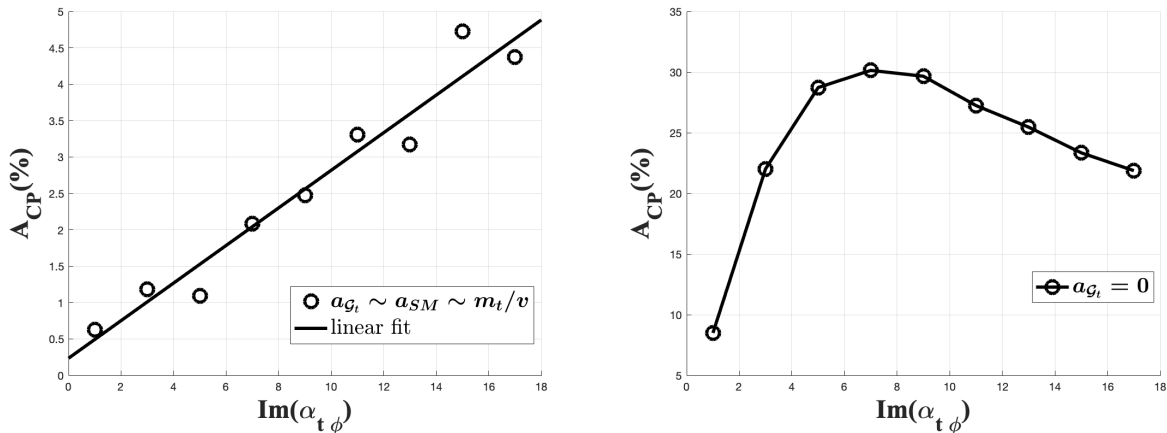


FIG. 2: The CP-Asymmetry as a function of the imaginary element of $\alpha_{t\phi}$, for $\Lambda = 1$ TeV. Left plot: the case of $a_{\mathcal{G}_t} \sim a_{SM} = m_t/v$ and $b_{\mathcal{G}_t} \sim \frac{v^2}{\Lambda^2} \cdot \text{Im}(\alpha_{t\phi})$. Right plot: the case where $a_{\mathcal{G}_t} = 0$ and $b_{\mathcal{G}_t} \sim \frac{v^2}{\Lambda^2} \cdot \text{Im}(\alpha_{t\phi})$. See text for more details.

coupling:

$$\mathcal{L}_{hZZ} = m_Z \cdot c_{hZZ} h Z^\mu Z_\mu, \quad (25)$$

and $c_{hZZ} = g_W m_Z / m_W$ in the SM. The CPC part of the differential cross-sections, $d\sigma_{CPV}^{t\bar{t}h}$, contains terms proportional to $a_{\mathcal{G}_t}^2$, $b_{\mathcal{G}_t}^2$, c_{hZZ}^2 and $a_{\mathcal{G}_t} \cdot c_{hZZ}$.

In Fig. 2 we plot the CP-Asymmetry \mathcal{A}_{CP} of Eq. 19, as a function of $\text{Im}(\alpha_{t\phi})$, the imaginary part of the Wilson coefficient of the operator $Q_{t\phi}$. For natural and weakly-interacting NP we expect $\alpha_{t\phi} \sim 1$ (for both the real and imaginary parts of $\alpha_{t\phi}$), so that for $\Lambda^2 \gg v^2$, we have for the scalar and pseudoscalar $t\bar{t}h$ couplings in Eq. 23:

$$a_{\mathcal{G}_t} \sim a_{SM} = O(1), \quad b_{\mathcal{G}_t} \sim O\left(\frac{v^2}{\Lambda^2}\right). \quad (26)$$

whence we expect (recall that $\mathcal{A}_{CP} \propto d\sigma_{CPV}^{t\bar{t}h} / d\sigma_{CPC}^{t\bar{t}h}$, see Eq. 6):

$$\mathcal{A}_{CP} \sim O\left(\frac{v^2}{\Lambda^2}\right) \sim O(1\%), \quad (27)$$

as indeed shown on the left panel in Fig. 2 for the case $\text{Im}(\alpha_{t\phi}) \sim 1$.

On the right panel of Fig. 2 we consider the case where the scalar $t\bar{t}h$ coupling vanishes, $a_{\mathcal{G}_t} = 0$ (these results also apply to the more general case where $a_{\mathcal{G}_t} \ll b_{\mathcal{G}_t}$). This is an unnatural choice for the parameter space of the SMEFT framework, but it could apply to model dependent scenarios with new particles of sub-TeV masses, such as the 2HDM, as was investigated in [23] (see also [14]). We see from Fig. 2 that, in such a case, a CP-Asymmetry of up to $\mathcal{A}_{CP} \sim 10 - 30\%$ is possible in $e^+e^- \rightarrow t\bar{t}h$, for $\text{Im}(\alpha_{t\phi}) \sim 1 - 10$ (note that $\text{Im}(\alpha_{t\phi}) \sim 20$ corresponds to a pseudo-scalar $t\bar{t}h$ coupling $b_{\mathcal{G}_t} \sim 1$).

B. Tree-level CPV from interference in top-Higgs associated production at the LHC

We consider here the expected sensitivity to potential CPV signals in scattering processes at the LHC, focusing again on the leading CPV effects within the SMEFT framework; namely, on the effects expected from the interference between the PTG operator $Q_{t\phi}$ and the SM. As before, a CP-odd phase $\propto \text{Im}(\alpha_{t\phi})$ is assumed to be present in the modified $t\bar{t}h$ interaction.

Let us first address the possibility of detecting CPV in $pp \rightarrow t\bar{t}h$, which is the LHC analog of the processes $e^+e^- \rightarrow t\bar{t}h$ described above. In contrast to e^+e^- colliders, $t\bar{t}h$ production at the LHC is dominated by the QCD gluon-gluon fusion process $gg \rightarrow t\bar{t}h$, which is CP-invariant at leading order even in the presence of the modified CPV $t\bar{t}h$ interaction of Eq. 20. As a consequence, the CPV asymmetry in $pp \rightarrow t\bar{t}h$ is too small to be detected at the

LHC. Specifically, as in the case of $e^+e^- \rightarrow t\bar{t}h$ described above, CPV in $pp \rightarrow t\bar{t}h$ is generated by interference of the Z -boson mediated electroweak (EW) processes $q\bar{q} \rightarrow Z \rightarrow t\bar{t}h$ where the Higgs is radiated from the Z -boson, with the diagrams where the Higgs is emitted from the top and/or anti-top quarks in this process, so the asymmetry is doubly suppressed: (i) by the ratio between the PDF's of the initial $q\bar{q}$ and gg states, i.e., $\text{PDF}(q\bar{q})/\text{PDF}(gg)$; and (ii) by a ratio of EW/QCD couplings. Unsurprisingly, a recent search by ATLAS [27], using dedicated CP-sensitive observables in $pp \rightarrow t\bar{t}h$, found no evidence for CPV.

Thus, to search for tree-level CPV effects at the LHC from the PTG operator $Q_{t\phi}$, one has to look for alternative scattering processes involving top-Higgs associated production. This leads us to consider the following two single-top plus Higgs production channels:

- **thW associated production:** $pp \rightarrow thW^-$ and the CC process $pp \rightarrow \bar{t}hW^+$, which are mediated by the gluon- b fusion processes $gb \rightarrow thW^-$ and $g\bar{b} \rightarrow \bar{t}hW^+$, respectively (see Fig. 3).
- **thj associated production:** $pp \rightarrow thj$ and the CC process $pp \rightarrow \bar{t}hj$, where j is a light quark or anti-quark jet, which are mediated by the q - b fusion processes $qb \rightarrow thj$ and $q\bar{b} \rightarrow \bar{t}hj$, respectively, where q is either an up-quark or down anti-quark; the leading effect is from u, d of the first generation (see Fig. 3).

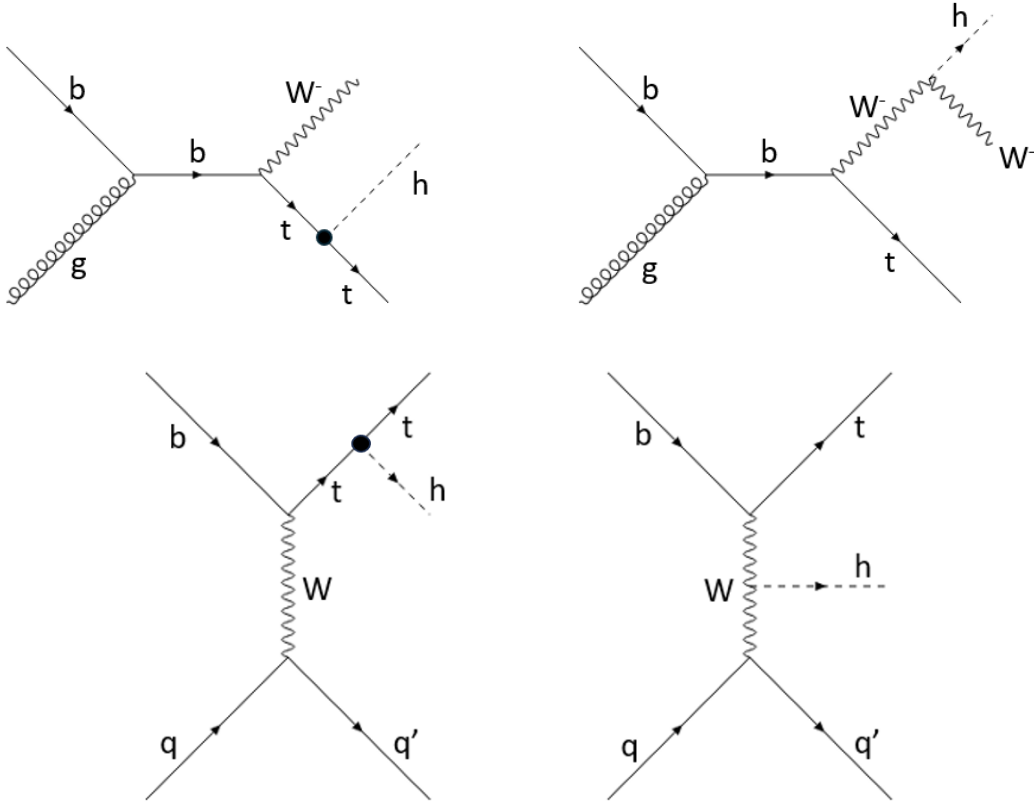


FIG. 3: Representative Feynman diagrams for the lowest order SM and NP contributions (marked by a heavy dot) to the $pp \rightarrow thW$ (upper diagrams) and $pp \rightarrow thj$ (lower diagrams) processes at the LHC. In each case, tree-level CP-violation arises from interference between the two diagrams. See also text.

Indeed, these top-Higgs associated production processes are at the focus of the ATLAS [26, 27] and CMS [28, 29] searches, due to their noticeable sensitivity to NP in general [30–32] and specifically to the tth Yukawa interaction [30, 33–39]. As shown below, they may also exhibit tree-level CPV from a CP-odd phase of the PTG operator $Q_{t\phi}$, via the interference between the diagram where the Higgs is radiated from the W -boson and the diagram where it is emitted from the top-quark.

It should also be noted that the total cross-section for each of the tH associated production processes is itself very sensitive to the interference between these two diagrams [30, 34, 35, 37–39]. Therefore, regardless of CPV, these two th production channels provide direct access to the size and sign of the tth Yukawa interaction, as their cross-sections can vary by more than an order of magnitude depending on the size and sign of the tth Yukawa coupling y_t (or

equivalently, on the size and sign of a_M in Eq. 20). We will show below that the CP asymmetry for these two th production channels is also sensitive to the sign (and size) of the scalar tth Yukawa coupling y_t .⁴

In order to assess the maximal size of a CPV effect in th associated production at the LHC due to a CP-odd phase in the tth Yukawa coupling from the operator $Q_{t\phi}$, i.e., the pseudo-scalar coupling $b_{\mathcal{G}_t}$ in Eq. 23, we will perform below a "sterile" analysis. In particular, we will not consider here the SM backgrounds to these processes (see e.g., [26–28]) and issues concerning the separation of the th signals from (the dominant) $pp \rightarrow t\bar{t}h$ process; in particular for the thW case [37, 39]. Also, we will not include the decays of the top-quark, of the Higgs and of the W – *boson* and the corresponding detection efficiencies. We emphasize, that such issues are expected to further dilute the expected CPV effect in th associated production reported below, and we leave them to a future work which will be dedicated to the investigation of CPV in single top + Higgs associated production at the LHC.

Let us now turn to the study of CPV effect in the aforementioned th associated production channels at the LHC. In analogy to the $e^+e^- \rightarrow t\bar{t}h$ case described in the previous section, the CPV parts of the differential hard cross-sections $gb \rightarrow thW$ and $qb \rightarrow thj$ are:

$$d\sigma_{CPV}^{thW,j} \propto m_t \cdot c_{hWW} \cdot b_{\mathcal{G}_t} \cdot \epsilon(p_b, p_t, p_h, p_{W-,j}) , \quad (28)$$

where $b_{\mathcal{G}_t}$ is the pseudo-scalar tth coupling in the SMEFT_t framework (see Eq. 23) and c_{hWW} represents the SM hWW coupling. For the CC channels, $g\bar{b} \rightarrow \bar{t}W^+h$ and $q\bar{b} \rightarrow \bar{t}hj$, replace $\epsilon(p_b, p_t, p_h, p_{W-}) \rightarrow \epsilon(p_{\bar{b}}, p_{\bar{t}}, p_h, p_{W+})$ and $\epsilon(p_b, p_t, p_h, p_j) \rightarrow \epsilon(p_{\bar{b}}, p_{\bar{t}}, p_h, p_{\bar{j}})$, respectively. Here also, the corresponding CPC part of the differential cross-sections contains terms proportional to $a_{\mathcal{G}_t}^2$, $b_{\mathcal{G}_t}^2$, c_{hWW}^2 and $a_{\mathcal{G}_t} \cdot c_{hWW}$.

TABLE IV: The expected CP asymmetries in $pp \rightarrow thW$ and $pp \rightarrow thj$ events, for $\Lambda = 1$ TeV, $\text{Im}(\alpha_{t\phi}) = 1$ and a tth Yukawa coupling $y_t = 0, \pm m_t/v$ (see Eq. 21). A selection cut was used on the c.m. energy $\sqrt{\hat{s}} < \Lambda$; see also text.

	$pp \rightarrow thW$			$pp \rightarrow thj$		
	$y_t = 0$	$y_t = m_t/v$	$y_t = -m_t/v$	$y_t = 0$	$y_t = m_t/v$	$y_t = -m_t/v$
\mathcal{A}_{CP}	0.2%	1.3%	0.1%	0.8%	1.7%	0.05%

TABLE V: The cross-sections $\sigma(pp \rightarrow thW) = \sigma(pp \rightarrow thW^-) = \sigma(pp \rightarrow \bar{t}hW^+)$, $\sigma(pp \rightarrow thj)$ and $\sigma(pp \rightarrow \bar{t}hj)$, at LO with $\Lambda = 1$ TeV, $\text{Im}(\alpha_{t\phi}) = 1$ and a selection $\sqrt{\hat{s}} < \Lambda$, for a tth Yukawa coupling $y_t = 0, \pm m_t/v$ (see Eq. 21).

	$y_t = 0$	$y_t = m_t/v$	$y_t = -m_t/v$
$\sigma(pp \rightarrow thW)$ [fb]	10.1	6.9	42.9
$\sigma(pp \rightarrow thj)$ [fb]	71.8	18.0	268.2
$\sigma(pp \rightarrow \bar{t}hj)$ [fb]	39.5	8.5	143.1

In Table IV we list the expected CP asymmetry \mathcal{A}_{CP} for the thW and thj signals at the LHC, for $\Lambda = 1$ TeV, $\text{Im}(\alpha_{t\phi}) = 1$ and for three values of the top-quark Yukawa coupling $y_t = 0, \pm m_t/v$. In Table V we list the corresponding leading order (LO) cross-sections. An upper selection cut $\sqrt{\hat{s}} < \Lambda$, i.e., on the center of mass energy of the hard processes, was applied on all event samples to ensure the validity of the EFT prescription.

The behaviour of \mathcal{A}_{CP} for these two processes as a function of $\text{Im}(\alpha_{t\phi})$, for $y_t = 0, \pm m_t/v$, is depicted in Fig. 4.⁵ As described in section III B, the CP-asymmetry \mathcal{A}_{CP} is constructed out of the T_N -odd observables, A_T, \bar{A}_T of Eqs. 17 and 18.

We observe three notable properties of the expected \mathcal{A}_{CP} in th associated production at the LHC:

- As expected (see above), for natural Wilson coefficients ($\text{Im}(\alpha_{t\phi}), \text{Re}(\alpha_{t\phi}) \sim 1$), the CP asymmetry is, at best, of $O(1\%)$. A naive estimate of the detection sensitivity to such an asymmetry, based on statistics only (see Eq. 14), shows that at least $O(10^5)$ $pp \rightarrow thW$ events would be required for a 3σ signal; this is not within the reach of the LHC.

⁴ Due to our focus on CPV we only consider the effects of the SMEFT operator $Q_{t\phi}$. A complete calculation of possible NP effects on other observables associated with these reactions required the inclusion of a number of other operators, see, e.g. [32].

⁵ The th event samples were generated using MADGRAPH5_AMC@NLO [40] at LO parton-level and with the SMEFTsim model of [15, 41] for the EFT framework. The 5-flavor scheme was used to generate all samples, with the NNPDF30_1o_as_0130 PDF set [42] and the default MADGRAPH5_AMC@NLO LO dynamical scale.

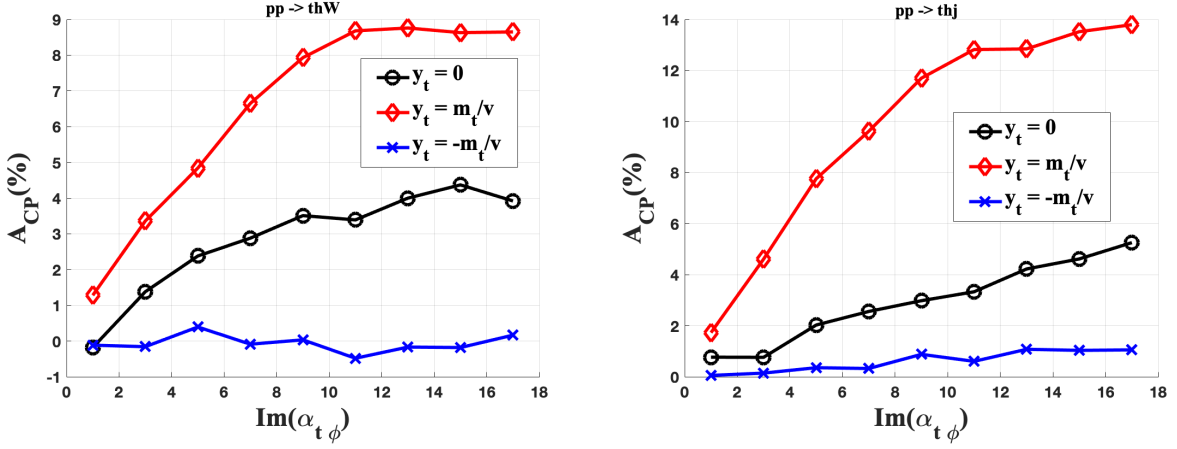


FIG. 4: The expected CP-asymmetries in thW (left) and thj (right) associated production at the LHC, as a function of the imaginary element of $\alpha_{t\phi}$, for $\Lambda = 1$ TeV and for $y_t = 0, \pm m_t/v$, respectively, where y_t is the tth Yukawa coupling (see Eq. 21). See also text.

- A sizable CP asymmetry, of $\mathcal{A}_{CP} \sim 10\%$, can arise only for $\text{Im}(\alpha_{t\phi}) \gtrsim 10$, which is unnaturally large within the EFT approach. However, as mentioned earlier, this case represents model-dependent scenarios of sub-TeV NP, e.g., multi-Higgs models, and not of multi-TeV (decoupling) NP scenarios.
- The strong interference effects noted previously, which depends on the size and sign of the top-quark Yukawa coupling, is clearly manifested also in \mathcal{A}_{CP} . In particular, the asymmetry is maximal in both the thW and thj channels, if $y_t = +m_t/v$ and it is strongly suppressed for $y_t = -m_t/v$. It is interesting to note that this behaviour of $\mathcal{A}_{CP}(y_t)$ is opposite to that of the cross-section, see Table V and [30, 34, 35, 37]; the reason is that the total (CP-conserving) cross-section appears in the denominator of \mathcal{A}_{CP} , see Eqs. 17-19.

V. TREE-LEVEL CPV IN TRI-LEPTON EVENTS FROM PURE NP DYNAMICS

In this section we will describe a case of a potential large tree-level CPV effect, of $O(10\%)$, from natural underlying NP which has $O(1)$ Wilson coefficients in the EFT prescription; this occurs within the TLCPV-III scenario defined in Sect. III A, when there is no (irreducible) SM tree-level contribution to the cross section. The results presented below are based on [25], where a more detailed analysis can be found.

Specifically, we consider the tri-lepton production at the LHC $ab \rightarrow \ell'^- \ell'^+ \ell^- + X$ and the CC channel $\bar{a}\bar{b} \rightarrow \ell'^+ \ell'^- \ell^+ + \bar{X}$. The underlying NP responsible for CPV in these tri-lepton signals at the LHC is assumed to correspond to the following two $t\ell\ell$ 4-Fermi effective operators [25]:⁶

$$Q_S = (\bar{\ell}_R \ell_R) (\bar{t}_R u_R), \quad Q_T = (\bar{\ell}_R \sigma_{\mu\nu} \ell_R) (\bar{t}_R \sigma_{\mu\nu} u_R); \quad \ell = e, \mu \quad (29)$$

and similarly for the $t\ell\ell$ 4-Fermi terms. The relevant Lagrangian is then

$$\mathcal{L} = \mathcal{L}_{SM} + \frac{1}{\Lambda^2} [(\alpha_S Q_S + \alpha_T Q_T) + \text{H.c.}], \quad (30)$$

These two operators (which correspond to the 4-Fermi operators $Q_{\ell equ}^{(1,3)}$ in Eq. 4) are not Hermitian, so, in general, their Wilson coefficients will contain CP-odd phases. Contributions from $Q_{S,T}$ can then interfere with each other (even if not with the SM), generating CPV effects. This indeed occurs in tri-lepton events at the LHC in the single-top production channels (see Fig. 5):

$$ug, gg \rightarrow \ell^+ \ell^- t, \ell^+ \ell^- t + j \quad (j = \text{light jet}) \quad (31)$$

⁶ We assume that the two operators have a common underlying scale, experimentally $\Lambda \gtrsim 1$ TeV, see [22].

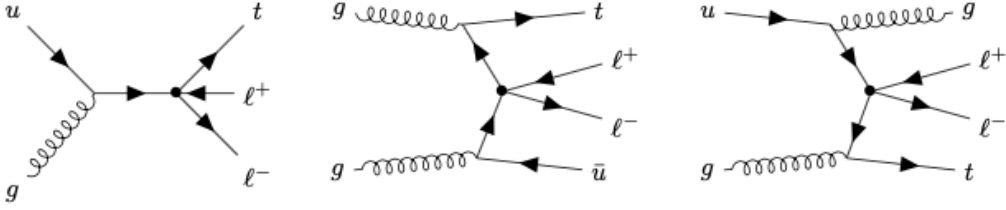


FIG. 5: Representative Feynman diagrams for the lowest order single top-quark + di-lepton production channels $pp \rightarrow t\ell^+\ell^-$ and $pp \rightarrow t\ell^+\ell^- + j$ (j is a light jet), via the $t\ell^+\ell^-$ 4-Fermi interaction (marked by a heavy dot).

and the CC counterparts (i.e., with \bar{t} in the final state).

Thus, considering CPV in the single-top production channels in Eq. 31, followed by the top decay to a charged lepton, we will focus, as an example, on the $e\mu\mu$ final state:⁷

$$\begin{aligned} pp &\rightarrow t\mu^+\mu^- + X \rightarrow e^+\mu^+\mu^- + X, \\ pp &\rightarrow \bar{t}\mu^+\mu^- + \bar{X} \rightarrow e^-\mu^-\mu^+ + \bar{X}, \end{aligned} \quad (32)$$

where the NP and CPV phases arise from the $t\mu\mu$ and/or $t\bar{c}\mu\mu$ 4-Fermi interactions in Eq. 30.

As was shown in [25], the dominant SM background to the inclusive tri-lepton production channels of Eq. 32 arises from WZ production, $pp \rightarrow WZ$, followed by the W and Z decays to charged leptons. The SM contributions to $pp \rightarrow e^+\mu^+\mu^- + X$ from other channels such as $pp \rightarrow t\bar{t}, t\bar{t}V, tVV, V + jets$ ($V = Z, W$) are much smaller [25]. In particular, there is no interference between the $t\mu\mu$ NP diagrams (see Fig. 5) and the SM contributions to the tri-leptons signal, so that the cross-section is of the form:

$$\sigma_{e\mu\mu}(m_{\mu\mu}^{min}) = \sigma_{e\mu\mu}^{SM}(m_{\mu\mu}^{min}) + \frac{\alpha^2}{\Lambda^4} \sigma_{e\mu\mu}^{NP}(m_{\mu\mu}^{min}), \quad (33)$$

where α^2 stands for all the NP \times NP coefficients (i.e., proportional to $|\alpha_S|^2$, $|\alpha_T|^2$ and $\alpha_S^*\alpha_T$) and we have defined the $m_{\mu\mu}^{min}$ -dependent cumulative cross-section, selecting events with $m_{\mu\mu} > m_{\mu\mu}^{min}$:

$$\sigma_{e\mu\mu}(m_{\mu\mu}^{min}) \equiv \sigma_{e\mu\mu}(m_{\mu\mu} > m_{\mu\mu}^{min}) = \int_{m_{\mu\mu} \geq m_{\mu\mu}^{min}} dm_{\mu\mu} \frac{d\sigma_{e\mu\mu}}{dm_{\mu\mu}}. \quad (34)$$

The invariant mass of the two muons in the final state, $m_{\mu\mu}$, turns out to be a useful discriminating parameter;⁸ the CP asymmetries are sensitive to the di-muons invariant mass, since the SM (which is dominant at low $m_{\mu\mu}$) contributes to the denominators while the CPV NP term (which is dominant for high $m_{\mu\mu}$) contributes to the numerators.

The CPV in this case is, therefore, a pure NP effect, since it arises from the imaginary part of the interference between the dimension 6 scalar and tensor operators, provided at least one of the corresponding Wilson coefficients is complex. In particular, the numerator of the CP-asymmetry \mathcal{A}_{CP} (and of the T_N -odd asymmetries A_T and \bar{A}_T) is proportional to the CPV part of the cross-section for $pp \rightarrow t\mu^+\mu^- \rightarrow e^+\mu^+\mu^- + X$:

$$d\sigma_{CPV} \propto \epsilon(p_{u_i}, p_{e^+}, p_{\mu^+}, p_{\mu^-}) \cdot \text{Im}(\alpha_S \alpha_T^*), \quad (35)$$

and similarly for the CC channel by replacing $\epsilon(p_{u_i}, p_{e^+}, p_{\mu^+}, p_{\mu^-})$ with $\epsilon(p_{\bar{u}_i}, p_{e^-}, p_{\mu^-}, p_{\mu^+})$.

We present below results for $|\alpha_S| = 1$, $|\alpha_T| = 0.25$ (which is motivated by the matching of the EFT framework to leptoquarks models, see [25]), with a maximal CP-odd phase for the $t\mu\mu$ and $t\bar{c}\mu\mu$ operators, so that the CPV coupling in Eq. 35 is set to:

$$\text{Im}(\alpha_S \cdot \alpha_T^*) = 0.25. \quad (36)$$

In Table ??, we list the resulting CPV and T_N -odd asymmetries for $m_{\ell\ell}^{min} = 400$ GeV, and in Fig. 6 we show the dependence of \mathcal{A}_{CP} on $m_{\ell\ell}^{min}$. Results are shown for both the ug -fusion and cg -fusion production channels, for

⁷ The processes in Eq. 31, followed by the top decay $t \rightarrow Wb \rightarrow \ell'\nu_{\ell'}b$, have interesting implications also for generic NP searches of new heavy states around the TeV scale, which can generate the top-leptons 4-Fermi contact terms $Q_{S,T}$ [22].

⁸ In the more general case of $pp \rightarrow \ell'^{\pm}\ell^{\pm}\ell^- + X$, we have $m_{\mu\mu} \rightarrow m_{\ell\ell}$ and $m_{\ell\ell}$ would be the invariant mass of the "none-top" opposite sign same-flavor (OSSF) di-leptons from the underlying hard process, i.e., of the di-leptons produced from the $t\ell\ell$ vertex and not from the top-quark decays.

$\Lambda = 1, 2$ TeV, and include SM effects background from $pp \rightarrow ZW^\pm + X$.

TABLE VI: The expected T_N -odd and CP asymmetries in tri-lepton events, $pp \rightarrow \ell^\pm \ell^+ \ell^- + X$, see text. Table taken from [25]

	ug -fusion: $\Lambda = 1(2)$ TeV	cg -fusion: $\Lambda = 1(2)$ TeV
\mathcal{A}_{CP}	11.1(7.9)%	3.9(0.7)%
A_T	16.4(13.5)%	3.1(0.5)%
\bar{A}_T	-5.8(-2.3)%	-4.7(-1.0)%

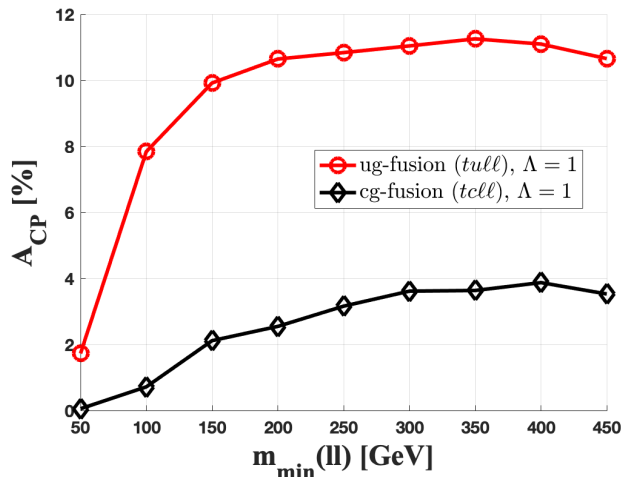


FIG. 6: The expected CP-asymmetry \mathcal{A}_{CP} , as a function of the invariant mass cut on the same-flavor di-leptons, see text. We are only showing central values, for more details see [25].

VI. SUMMARY

We have systematically analysed the discovery potential of CP-violation searches in scattering processes at TeV-scale colliders, parametrizing the underlying heavy NP in an effective field theory framework and using the SMEFT basis for the higher dimensional operators.

We have based our methodology on naturality arguments and possible structures of the potential heavy physics that underlies the SM, which is assumed to be weakly interacting and decoupling. We have then considered the phenomenological implications of the CP-violating sector of the SMEFT framework in three limiting cases: (i) an enhanced $U(3)^5$ flavour symmetry that the SM possesses when all fermion masses are set to zero, (ii) a reduced $U(3)^4$ flavour symmetry where top-quark mass effects are included and (iii) no flavour symmetry.

In particular, we have spelled out guiding principles for the hunt of CPV in high-energy scattering processes, finding that if flavor changing interactions are suppressed (or absent) in the underlying heavy physics, then the leading CPV signals are expected from a single dim.6 operator that involves the top-quark and Higgs fields, $Q_{t\phi} = \phi^\dagger \phi (\bar{q}_3 t) \tilde{\phi}$, which modifies the tth Yukawa coupling. We showed, however, that for a natural underlying NP with $O(1)$ couplings, CPV effects from this top-Higgs operator are expected to be too small - below the expected sensitivity of the LHC and other future high-energy colliders, unless there is yet-undiscovered physics in the sub-TeV region.

We thus conclude that, under the naturality condition of the underlying heavy theory, a measurable CP-violating effect can arise in high-energy scattering processes *only* in case (iii) mentioned above, where the NP has sizable, $O(1)$, flavor-changing interactions and the CPV signal is generated purely in the NP sector, i.e., from NP \times NP effects and not from SM \times NP interference.

We provide several examples that illustrate our general conclusions, by studying potential CPV from NP physics in $e^+e^- \rightarrow t\bar{t}h$ at a future high-energy e^+e^- collider and in top-Higgs associated production at the LHC via $pp \rightarrow$

thW, thj .

-
- [1] A. D. Sakharov. Violation of CP Invariance, C asymmetry, and baryon asymmetry of the universe. *Pisma Zh. Eksp. Teor. Fiz.*, 5:32–35, 1967.
- [2] V. A. Kuzmin, V. A. Rubakov, and M. E. Shaposhnikov. On the Anomalous Electroweak Baryon Number Nonconservation in the Early Universe. *Phys. Lett. B*, 155:36, 1985.
- [3] G. C. Branco, R. Gonzalez Felipe, and F. R. Joaquim. Leptonic CP Violation. *Rev. Mod. Phys.*, 84:515–565, 2012, 1111.5332.
- [4] S. Navas et al. (Particle Data Group). CP Violation in the Quark Sector. *Phys. Rev. D*, 110:030001, 2024.
- [5] V. A. Rubakov and M. E. Shaposhnikov. Electroweak baryon number nonconservation in the early universe and in high-energy collisions. *Usp. Fiz. Nauk*, 166:493–537, 1996, hep-ph/9603208.
- [6] Werner Bernreuther. CP violation and baryogenesis. *Lect. Notes Phys.*, 591:237–293, 2002, hep-ph/0205279.
- [7] Laurent Canetti, Marco Drewes, and Mikhail Shaposhnikov. Matter and Antimatter in the Universe. *New J. Phys.*, 14:095012, 2012, 1204.4186.
- [8] W. Buchmuller and D. Wyler. Effective Lagrangian Analysis of New Interactions and Flavor Conservation. *Nucl. Phys.*, B268:621–653, 1986.
- [9] C. Arzt, M. B. Einhorn, and J. Wudka. Patterns of deviation from the standard model. *Nucl. Phys.*, B433:41–66, 1995, hep-ph/9405214.
- [10] Martin B. Einhorn and Jose Wudka. The Bases of Effective Field Theories. *Nucl. Phys.*, B876:556–574, 2013, 1307.0478.
- [11] B. Grzadkowski, M. Iskrzynski, M. Misiak, and J. Rosiek. Dimension-Six Terms in the Standard Model Lagrangian. *JHEP*, 10:085, 2010, 1008.4884.
- [12] Ilaria Brivio and Michael Trott. The Standard Model as an Effective Field Theory. *Phys. Rept.*, 793:1–98, 2019, 1706.08945.
- [13] Martin B. Einhorn and Jose Wudka. The Bases of Effective Field Theories. *Nucl. Phys. B*, 876:556–574, 2013, 1307.0478.
- [14] David Atwood, Shaouly Bar-Shalom, Gad Eilam, and Amarjit Soni. CP violation in top physics. *Phys. Rept.*, 347:1–222, 2001, hep-ph/0006032.
- [15] Ilaria Brivio. SMEFTsim 3.0 — a practical guide. *JHEP*, 04:073, 2021, 2012.11343.
- [16] Céline Degrande and Julien Touchèque. A reduced basis for CP violation in SMEFT at colliders and its application to diboson production. *JHEP*, 04:032, 2022, 2110.02993.
- [17] Quentin Bonnefoy, Emanuele Gendy, Christophe Grojean, and Joshua T. Ruderman. Beyond Jarlskog: 699 invariants for CP violation in SMEFT. *JHEP*, 08:032, 2022, 2112.03889.
- [18] Anson Hook. TASI Lectures on the Strong CP Problem and Axions. *PoS*, TASI2018:004, 2019, 1812.02669.
- [19] G. D’Ambrosio, G. F. Giudice, G. Isidori, and A. Strumia. Minimal flavor violation: An Effective field theory approach. *Nucl. Phys. B*, 645:155–187, 2002, hep-ph/0207036.
- [20] Gino Isidori and David M. Straub. Minimal Flavour Violation and Beyond. *Eur. Phys. J. C*, 72:2103, 2012, 1202.0464.
- [21] Jonathan Kley, Tobias Theil, Elena Venturini, and Andreas Weiler. Electric dipole moments at one-loop in the dimension-6 SMEFT. *Eur. Phys. J. C*, 82(10):926, 2022, 2109.15085.
- [22] Yoav Afik, Shaouly Bar-Shalom, Amarjit Soni, and Jose Wudka. New flavor physics in di- and trilepton events from single-top production at the LHC and beyond. *Phys. Rev. D*, 103(7):075031, 2021, 2101.05286.
- [23] S. Bar-Shalom, D. Atwood, G. Eilam, R. R. Mendel, and A. Soni. Large tree level CP violation in $e^+e^- \rightarrow t\bar{t}H^0$ in the two Higgs doublet model. *Phys. Rev. D*, 53:1162–1167, 1996, hep-ph/9508314.
- [24] S. Bar-Shalom, D. Atwood, and A. Soni. Two Higgs doublets models and CP violating Higgs exchange in $e^+e^- \rightarrow t$ anti- t Z . *Phys. Lett. B*, 419:340–347, 1998, hep-ph/9707284.
- [25] Yoav Afik, Shaouly Bar-Shalom, Kuntal Pal, Amarjit Soni, and Jose Wudka. Generic Tests of CP Violation in High-pT Multilepton Signals at the LHC and Beyond. *Phys. Rev. Lett.*, 131(17):171801, 2023, 2212.09433.
- [26] Georges Aad et al. CP Properties of Higgs Boson Interactions with Top Quarks in the $t\bar{t}H$ and tH Processes Using $H \rightarrow \gamma\gamma$ with the ATLAS Detector. *Phys. Rev. Lett.*, 125(6):061802, 2020, 2004.04545.
- [27] Georges Aad et al. Probing the CP nature of the top–Higgs Yukawa coupling in $t\bar{t}H$ and tH events with $H \rightarrow b\bar{b}$ decays using the ATLAS detector at the LHC. *Phys. Lett. B*, 849:138469, 2024, 2303.05974.
- [28] Armen Tumasyan et al. Search for CP violation in $t\bar{t}H$ and tH production in multilepton channels in proton-proton collisions at $\sqrt{s} = 13$ TeV. *JHEP*, 07:092, 2023, 2208.02686.
- [29] Albert M Sirunyan et al. Measurements of $t\bar{t}H$ Production and the CP Structure of the Yukawa Interaction between the Higgs Boson and Top Quark in the Diphoton Decay Channel. *Phys. Rev. Lett.*, 125(6):061801, 2020, 2003.10866.
- [30] Marco Farina, Christophe Grojean, Fabio Maltoni, Ennio Salvioni, and Andrea Thamm. Lifting degeneracies in Higgs couplings using single top production in association with a Higgs boson. *JHEP*, 05:022, 2013, 1211.3736.
- [31] Céline Degrande, Fabio Maltoni, Ken Mimasu, Eleni Vryonidou, and Cen Zhang. Single-top associated production with a Z or H boson at the LHC: the SMEFT interpretation. *JHEP*, 10:005, 2018, 1804.07773.
- [32] Subhaditya Bhattacharya, Sanjoy Biswas, Kuntal Pal, and Jose Wudka. Associated production of Higgs and single top at the LHC in presence of the SMEFT operators. *JHEP*, 08:015, 2023, 2211.05450.
- [33] F. Maltoni, K. Paul, T. Stelzer, and S. Willenbrock. Associated production of Higgs and single top at hadron colliders. *Phys. Rev. D*, 64:094023, 2001, hep-ph/0106293.

- [34] Sanjoy Biswas, Emidio Gabrielli, and Barbara Mele. Single top and Higgs associated production as a probe of the Htt coupling sign at the LHC. *JHEP*, 01:088, 2013, 1211.0499.
- [35] Federico Demartin, Fabio Maltoni, Kentarou Mawatari, and Marco Zaro. Higgs production in association with a single top quark at the LHC. *Eur. Phys. J. C*, 75(6):267, 2015, 1504.00611.
- [36] Lei Wu. Enhancing thj Production from Top-Higgs FCNC Couplings. *JHEP*, 02:061, 2015, 1407.6113.
- [37] Federico Demartin, Benedikt Maier, Fabio Maltoni, Kentarou Mawatari, and Marco Zaro. tWH associated production at the LHC. *Eur. Phys. J. C*, 77(1):34, 2017, 1607.05862.
- [38] Vernon Barger, Kaoru Hagiwara, and Ya-Juan Zheng. Probing the top Yukawa coupling at the LHC via associated production of single top and Higgs. *JHEP*, 09:101, 2020, 1912.11795.
- [39] Henning Bahl, Philip Bechtle, Sven Heinemeyer, Judith Katzy, Tobias Klingl, Krisztian Peters, Matthias Saimpert, Tim Stefaniak, and Georg Weiglein. Indirect \mathcal{CP} probes of the Higgs-top-quark interaction: current LHC constraints and future opportunities. *JHEP*, 11:127, 2020, 2007.08542.
- [40] Johan Alwall, Michel Herquet, Fabio Maltoni, Olivier Mattelaer, and Tim Stelzer. MadGraph 5 : Going Beyond. *JHEP*, 06:128, 2011, 1106.0522.
- [41] Ilaria Brivio, Yun Jiang, and Michael Trott. The SMEFTsim package, theory and tools. *JHEP*, 12:070, 2017, 1709.06492.
- [42] Richard D. Ball et al. Parton distributions for the LHC Run II. *JHEP*, 04:040, 2015, 1410.8849.